

**STUDY OF HALL AND SORET EFFECT ON MHD FLOW WITH A RAMPED
PLATE TEMPERATURE OF AN EXPONENTIALLY ACCELERATED VERTICAL
PLATE EMBEDDED IN A POROUS MEDIUM**

U.S.Rajput and M.Shareef*

Department of Mathematics and Astronomy, University of Lucknow, Lucknow-226007, India

Received: 05 October 2018 / Accepted: 21 December 2018 / Published online: 01 January 2019

ABSTRACT

The present literature deals with the study of MHD flow of an incompressible viscous electrically conducting fluid along an exponentially accelerated infinite vertical plate in a rotating system. The effects of thermodiffusion, thermal radiation and Hall current, are analysed with ramped and isothermal plate conditions. The non-dimensional coupled partial differential equations of the model are solved analytically by using Laplace Transform method with the help of Heaviside step function; thus the expression for velocity field, temperature field, concentration field, skin friction coefficient, Nusselt number and Sherwood number are obtained. The influence of physical parameters such as m (Hall parameter), S_r (Soret number), K (Darcy permeability), λ (exponential parameter), Ω (rotation parameter) and R (radiation parameter) on these fields are discussed in detail through graphs.

Keywords: Soret effect; Hall current; Rotation; Radiation.

Author Correspondence, e-mail: rajputshareeflu@gmail.com

doi: <http://dx.doi.org/10.4314/jfas.v11i1.25>



1. INTRODUCTION

Previously, some valuable researches have been done in the area of MHD flow due to its great applications in the field of science and engineering such as MHD generators, nuclear reactors, induction pumps, space vehicle propulsion and oil exploration. The thermo-physical properties of flow of electrically conducting fluids can be controlled by imposing the magnetic force on the flow (Agarwal *et al.* [1], Muthucumaraswamy and Prema [19], Jaimala *et al.* [13], Mazumdar *et al.* [18], Branover [6], Cowling [8], Osalusi and Sibanda [22]). The governing partial differential equations of the model are non linear but general behaviour can be studied by simplify the problem taking some assumptions.

Moreover, flow through a porous medium have plentiful geophysical and engineering applications, for example, in chemical engineering for purification and filtration process; in petroleum technology to understand the movement of natural gas, oil and water through the oil reservoirs; in agriculture engineering to analyze the underground water resources. By virtue of these big applications, a number of researchers have studied MHD free convective flow with heat and mass transfer in a porous medium; a few of them are Kim [15], Makinde and Mhone [17], Sattar [32], Raptis and Kafousias [31], Soundalgekar [35], Muthucumaraswamy *et al.* [21].

Also, at a high operating temperature, thermal radiation has some significant effect on the flow behavior of electrically conducting fluid. A fluid at high temperature generates heat by thermal radiation and the radiation energy mechanism of the fluid: (Takhar *et al.* [36], Ganesan and Laganathan [9], Raptis [29], Chamkha [7], Takhar *et al.* [37]). Hossain and Takhar [11] investigated the Radiation effect on mixed convection along a vertical plate with uniform surface temperature. Also, the radiation effect on unsteady MHD flow of a viscous electrically conducting fluid past a plane surface was studied by Raptis and Massalas [30]. Prasad *et al.* [27] analyzed the Radiation and mass transfer effects on two-dimensional flow past an impulsively started infinite vertical plate. They found out that an increase in the radiation parameter can decrease the temperature as well as velocity of the fluid in the boundary layer region. Similarly, the rotating fluids have their abundant astrophysical and geophysical applications. Some natural phenomena such as ocean circulations currents,

geophysical systems, hurricanes tornadoes, etc. imply rotating flows with heat and mass transfer. Several books and articles on heat transfer and hydrodynamic characteristics of rotating flows have been published: (Greenspan [10], Owen and Rogers [23], Soong and Ma [34], Soong [33], Muthucumaraswamy *et al.* [20]).

Further, due to temperature gradient different types of particle move differently. So, the temperature gradient can also generate the concentration flux inside the fluid and this phenomenon is known as the (Thermophoresis) Soret effect (Platten [24]). Kafoussias and Williams [14] subsequently studied the Dufour and Soret effects on the mixed convective and mass transfer steady laminar boundary layer flow, with temperature dependent viscosity, over a vertical flat plate. A numerical solution of oscillatory chemically-reacting MHD natural convection double-diffusive boundary layers in a porous medium with Soret and Dufour effects was studied by Bhargava *et al.* [5]. Postelnicu [25] analyzed the Soret and Dufour effects on MHD flow with heat and mass transfer by natural convection from vertical surface in a porous medium. Further, Postelnicu [26] worked on the influence of chemical reaction on heat and mass transfer by free convection from vertical surface in porous media considering the Soret and Dufour effects. The Soret and Dufour effects on convective flow past a vertical porous plate with variable suction was investigated by Alam and Rahman [2]. Some research papers related to Soret effect have been published by Beg *et al.* [4], Anghel [3], Makinde [16] and Ibrahim [12].

Influenced by the above-discussed literature and applications, we extended our previous work [28] to study the Soret effect on MHD flow near the exponentially accelerated infinite vertical plate in a rotating system through a porous medium with radiation. The governing partial differential equations of the model have been solved analytically by using the Laplace transform method. The effect of various parameters involved in the problem on velocity, temperature and concentration are presented and discussed graphically.

2. MATHEMATICAL FORMULATION AND SOLUTION

Let us consider a coordinate system such that an infinite plate is lying in $z=0$ plane and a magnetic field \vec{B} is applied normal to the plate. Both the plate and fluid are in a state of rigid

body rotation with uniform angular velocity $\vec{\Omega} = (0, 0, \Omega)$ about z - axis. Initially, the plate is at rest having a uniform temperature T_∞ and concentration C_∞ . At time $t > 0$, the plate is suddenly begins to move vertically upward in its own plane in positive x direction with a velocity $u_0 e^{-\lambda t}$ and concentration are lowered or raised to C_p . At the same time the plate temperature is changed to \bar{T}_p ($0 < t < t_0$) and T_p ($t \geq t_0$). The movement of the plate and the free convection causes the fluid motion. The governing PDEs of the models are non-linear but general characteristics of the fluid motion within the boundary layer can be analysed by simplified problem with some assumptions.

- i) All the fluid properties are constants and the variation in density is neglected everywhere except in the buoyancy term.
- ii) In the generalized Ohm's law, effect of Hall currents is taken into account and thermoelectric effect and ion-slip are neglected.
- iii) The fluid far away from the plate is undisturbed.
- iv) The fluid has small value of magnetic Reynolds number; hence the induced magnetic field can be neglected.
- v) No polarization or applied voltages exist.
- vi) The plate is of infinite extent so all the physical variables can be considered as a function of t and z only.
- vii) The plate is electrically non-conducting.

The governing equations of a viscous, incompressible and electrically conducting fluid under the above made assumptions are:

Momentum transport equation

$$\frac{\partial u}{\partial t} - 2\Omega v = \nu \frac{\partial^2 u}{\partial z^2} + g\beta(T - T_\infty) + g\beta^*(C - C_\infty) + \frac{\sigma B_o^2}{\rho} \frac{(m v - u)}{1 + m^2} - \frac{\nu}{K} u \quad (1)$$

$$\frac{\partial v}{\partial t} + 2\Omega u = \nu \frac{\partial^2 v}{\partial z^2} - \frac{\sigma B_o^2}{\rho} \frac{(v + m u)}{1 + m^2} - \frac{\nu}{K} v \quad (2)$$

Energy transport equation

$$\frac{\partial T}{\partial t} = \frac{k}{\rho c_p} \frac{\partial^2 T}{\partial z^2} - \frac{1}{\rho c_p} \frac{\partial q^{(v)}}{\partial z} \tag{3}$$

Mass transport equation

$$\frac{\partial C}{\partial t} = D \frac{\partial^2 C}{\partial z^2} + \frac{D_T k_T}{T_m} \frac{\partial^2 T}{\partial z^2} \tag{4}$$

The admissible initial and boundary conditions are taken as

$$\left. \begin{aligned} t \leq 0 : u(z, t) = 0, v(z, t) = 0, T(z, t) = T_\infty, C(z, t) = C_\infty; \\ t > 0 : u(0, t) = u_o e^{-\lambda t} (\lambda \geq 0), v(0, t) = 0, C(0, t) = C_\infty, T(0, t) = \begin{cases} \bar{T}_p, & t < t_o \\ T_p, & t \geq t_o \end{cases} \\ \text{and } u(z, t) \rightarrow 0, v(z, t) \rightarrow 0, T(z, t) \rightarrow T_\infty, C(z, t) \rightarrow C_\infty \text{ as } z \rightarrow \infty; \end{aligned} \right\} \tag{5}$$

where $\bar{T}_p = T_\infty + (T_p - T_\infty) \frac{t}{t_o}$ and $t_o = \frac{v}{u_o^2}$.

Taking Rosseland approximation (Prasad et al. (2007)), the radiative heat flux $q^{(v)}$ takes the form

$$q^{(v)} = -\frac{4\sigma_s}{3k_e} \frac{\partial T^4}{\partial z} \tag{6}$$

within the flow, the temperature difference is sufficiently small, so that T^4 can be approximated using Taylor series about $T = T_\infty$ (neglecting higher order terms) i.e.

$$T^4 \cong 4T_\infty^3 T - 3T_\infty^4 \tag{7}$$

with the help of (6) and (7), (3) takes form

$$\frac{\partial T}{\partial t} = \alpha \frac{\partial^2 T}{\partial z^2} + \frac{16\sigma_s \alpha T_\infty^3}{3k_e k} \frac{\partial^2 T}{\partial z^2} \tag{8}$$

For converting the equation into dimensionless form, we use the following non-dimensional parameters and variables

$$\left. \begin{aligned} u' &= \frac{u}{u_o}, v' = \frac{v}{u_o}, t' = \frac{u_o^2}{\nu} t, z' = \frac{u_o}{\nu} z, \theta = \frac{(T - T_\infty)}{(T_p - T_\infty)}, \phi = \frac{(C - C_\infty)}{(C_p - C_\infty)}, R = \frac{k_e k}{4\sigma_s T_o^3}, \\ S_c &= \frac{\nu}{D}, P_r = \frac{\nu}{\alpha}, \lambda' = \frac{\nu}{u_o^2} \lambda, M = \frac{\sigma B_o^2 \nu}{\rho u_o^2}, \Omega' = \frac{\nu}{u_o^2} \Omega, K' = \frac{u_o^2}{\nu^2} K, \\ G_r &= \frac{g\beta\nu(T_p - T_\infty)}{u_o^3}, G_m = \frac{g\beta^* \nu(C_p - C_\infty)}{u_o^3}, S_r = \frac{D_T k_T (T_s - T_\infty)}{T_m \nu (C_s - C_\infty)}. \end{aligned} \right\} \quad (9)$$

Equations (1), (2), (4), (5) and (8), by using equation (9), reduce to

$$\frac{\partial u'}{\partial t'} - 2\Omega' v' = \frac{\partial^2 u'}{\partial z'^2} + \frac{M}{1+m^2} (m v' - u') + G_r \theta + G_m \phi - \frac{u'}{K'} \quad (10)$$

$$\frac{\partial v'}{\partial t'} + 2\Omega' u' = \frac{\partial^2 v'}{\partial z'^2} - \frac{M}{1+m^2} (v' + m u') - \frac{v'}{K'} \quad (11)$$

$$\frac{\partial \theta}{\partial t'} = \frac{1}{R_a P_r} \frac{\partial^2 \theta}{\partial z'^2} \quad (12)$$

$$\frac{\partial \phi}{\partial t'} = \frac{1}{S_c} \frac{\partial^2 \phi}{\partial z'^2} + S_r \frac{\partial^2 \theta}{\partial z'^2} \quad (13)$$

$$\left. \begin{aligned} t' \leq 0 : u'(z', t') &= 0, v'(z', t') = 0, \theta(z', t') = 0, \phi(z', t') = 0; \\ t' > 0 : u'(0, t') &= e^{-\lambda' t'} (\lambda' \geq 0), v'(0, t') = 0, \phi(0, t') = 1, \theta(0, t') = \begin{cases} t', & t' \leq 1 \\ 1, & t' > 1 \end{cases} \\ \text{and } u'(z', t') \rightarrow 0, v'(z', t') \rightarrow 0, \theta(z', t') \rightarrow 0, \phi(z', t') \rightarrow 0 &\text{ as } z' \rightarrow \infty. \end{aligned} \right\} \quad (14)$$

Now combine equations (10) and (11), we get,

$$\frac{\partial V'}{\partial t'} = \frac{\partial^2 V'}{\partial z'^2} - bV' + G_r \theta + G_m \phi \quad (15)$$

where $V' = u' + iv'$ and $i = \sqrt{-1}$.

Equation (14) changes as:

$$\left. \begin{aligned} t' \leq 0: V'(z', t') = 0, \theta(z', t') = 0, \phi(z', t') = 0; \\ t' > 0: V'(0, t') = e^{-\lambda t'}, \phi(0, t') = 1, \theta(0, t') = \begin{cases} t', & t' \leq 1 \\ 1, & t' > 1 \end{cases} \end{aligned} \right\} \tag{16}$$

and $V'(z', t') \rightarrow 0, \theta(z', t') \rightarrow 0, \phi(z', t') \rightarrow 0$ as $z' \rightarrow \infty$.

After removing prime ('), above set of equations reduce to

$$\frac{\partial V}{\partial t} = \frac{\partial^2 V}{\partial z^2} - bV + G_r \theta + G_m \phi \tag{17}$$

$$\frac{\partial \theta}{\partial t} = \frac{1}{R_a P_r} \frac{\partial^2 \theta}{\partial z^2} \tag{18}$$

$$\frac{\partial \phi}{\partial t} = \frac{1}{S_c} \frac{\partial^2 \phi}{\partial z^2} + S_r \frac{\partial^2 \theta}{\partial z^2} \tag{19}$$

with boundary conditions

$$\left. \begin{aligned} t \leq 0: V(z, t) = 0, \theta(z, t) = 0, \phi(z, t) = 0; \\ t > 0: V(0, t) = e^{-\lambda t}, \phi(0, t) = 1, \theta(0, t) = \begin{cases} t, & t \leq 1 \\ 1, & t > 1 \end{cases} \end{aligned} \right\} \tag{20}$$

and $V(z, t) \rightarrow 0, \theta(z, t) \rightarrow 0, \phi(z, t) \rightarrow 0$ as $z \rightarrow \infty$.

Laplace transform method is used to solve the equations (17), (18) and (19) with conditions prescribed in equation (20). Therefore, after applying the Laplace transform to the equations (17), (18), (19) and using initial conditions, we get a set of equations in (z, s) as follows:

$$\frac{d^2}{dz^2} \bar{\theta}(z, s) - R_a P_r s \bar{\theta}(z, s) = 0 \tag{21}$$

$$\frac{d^2}{dz^2} \bar{\phi}(z, s) - S_c s \bar{\phi}(z, s) = -S_c S_r \frac{\partial^2 \bar{\theta}(z, s)}{dz^2} \tag{22}$$

$$\frac{d^2}{dz^2} \bar{V}(z, s) - (b + s) \bar{V}(z, s) = -G_r \bar{\theta}(z, s) - G_m \bar{\phi}(z, s) \tag{23}$$

Under the changed boundary conditions

$$\bar{V}(0, s) = \frac{1}{s + \lambda}, \bar{V}(\infty, s) = 0 \tag{24}$$

$$\bar{\theta}(0, s) = \frac{1 - e^{-s}}{s^2}, \bar{\theta}(\infty, s) = 0 \tag{25}$$

$$\bar{\phi}(0, s) = \frac{1}{s}, \bar{\phi}(\infty, s) = 0 \tag{26}$$

where Laplace transform of $V(z, t)$, $\theta(z, t)$ and $\phi(z, t)$ are denoted as $\bar{V}(z, s)$, $\bar{\theta}(z, s)$ and $\bar{\phi}(z, s)$ respectively.

By using equation (25) into equation (21), we get,

$$\bar{\theta}(z, s) = \frac{(1 - e^{-s})}{s^2} e^{-z\sqrt{sp_r R_a}} \tag{27}$$

Using the property; If $L^{-1}\{F(s)\} = f(t)$ then $L^{-1}\{e^{-ns} F(s)\} = f(t - n)H(t - n)$, the equation (27)

gives the temperature profile as follows

$$\theta(z, t) = \theta_1(z, t) - \theta_1(z, t - 1)H(t - 1), \tag{28}$$

where

$$\theta_1(z, t) = L^{-1} \left\{ \frac{e^{-z\sqrt{sp_r R_a}}}{s^2} \right\} = -ze^{-\frac{z^2 P_r R_a}{4t}} \frac{\sqrt{t P_r R_a}}{\sqrt{\pi}} + \left(t + \frac{z^2 P_r R_a}{2} \right) Erfc \left(\frac{z\sqrt{P_r R_a}}{2\sqrt{t}} \right),$$

here $H(t - 1)$ is the Heaviside step function, L^{-1} indicates the inverse Laplace transform and $Erfc(\cdot) = 1 - Erf(\cdot)$ is the complimentary error function.

Now for finding the concentration profile, putting equation (27) into equation (22) and using the boundary conditions (26), we get

$$\bar{\phi}(z, s) = \left(\frac{e^{-z\sqrt{sS_c}}}{s} \right) + a \frac{(1 - e^{-s})}{s^2} \left(e^{-z\sqrt{sp_r R_a}} - e^{-z\sqrt{sS_c}} \right) \tag{29}$$

$$\text{or } \phi(z, t) = L^{-1} \left(\frac{e^{-z\sqrt{sS_c}}}{s} \right) + aL^{-1} \left(\frac{e^{-z\sqrt{sp_r R_a}} - e^{-z\sqrt{sS_c}}}{s^2} \right) - aL^{-1} \left\{ e^{-s} \left(\frac{e^{-z\sqrt{sp_r R_a}} - e^{-z\sqrt{sS_c}}}{s^2} \right) \right\}$$

$$\text{or } \phi(z, t) = Erfc \left(\frac{z\sqrt{S_c}}{2\sqrt{t}} \right) + a\phi_1(z, t) - a\phi_1(z, t - 1)H(t - 1), \tag{30}$$

here
$$\phi_1(z, t) = L^{-1} \left(\frac{e^{-z\sqrt{sP_rR_a}} - e^{-z\sqrt{sS_c}}}{s^2} \right) = - \left(t + z^2 \frac{S_c}{2} \right) \text{Erfc} \left(\frac{z\sqrt{S_c}}{2\sqrt{t}} \right) - z\sqrt{\frac{t}{\pi}} \left(e^{-\frac{z^2P_rR_a}{4t}} \sqrt{P_rR_a} - e^{-\frac{z^2P_rR_a}{4t}} \sqrt{S_c} \right) + \left(t + \frac{z^2P_rR_a}{2} \right) \text{Erfc} \left(\frac{z\sqrt{P_rR_a}}{2\sqrt{t}} \right).$$

By putting equation (27) and (29) into equation (23) and using the boundary conditions (24), we get the velocity profile as follows:

$$\bar{V}(z, s) = \frac{e^{-z\sqrt{b+s}}}{s + \lambda} + \frac{A_3}{s(s - B_2)} \left(e^{-z\sqrt{sS_c}} - e^{-z\sqrt{b+s}} \right) + \frac{1 - e^{-s}}{s^2} \frac{(A_1 + A_2)}{(s - B_1)} \left(e^{-z\sqrt{R_aP_r}} - e^{-z\sqrt{b+s}} \right) + \frac{1 - e^{-s}}{s^2} \frac{aA_3}{(s - B_2)} \left(e^{-z\sqrt{b+s}} - e^{-z\sqrt{sS_c}} \right)$$

or
$$V(z, t) = L^{-1} \left\{ \frac{e^{-z\sqrt{b+s}}}{s + \lambda} + \frac{A_3}{s(s - B_2)} \left(e^{-z\sqrt{sS_c}} - e^{-z\sqrt{b+s}} \right) \right\} + L^{-1} \left\{ \frac{aA_3}{s^2(s - B_2)} \left(e^{-z\sqrt{b+s}} - e^{-z\sqrt{sS_c}} \right) \right\} + L^{-1} \left\{ \frac{(A_1 + A_2)}{s^2(s - B_1)} \left(e^{-z\sqrt{R_aP_r}} - e^{-z\sqrt{b+s}} \right) \right\} - L^{-1} \left[e^{-s} \left\{ \frac{(A_1 + A_2)}{s^2(s - B_1)} \left(e^{-z\sqrt{R_aP_r}} - e^{-z\sqrt{b+s}} \right) \right\} \right] - L^{-1} \left[e^{-s} \left\{ \frac{aA_3}{s^2(s - B_2)} \left(e^{-z\sqrt{b+s}} - e^{-z\sqrt{sS_c}} \right) \right\} \right]$$

or

$$V(z, t) = c_1 \{ 2\cosh(k_1z) + e^{-k_1z} \text{Erf}(k_1\sqrt{t} - \eta) - e^{k_1z} \text{Erf}(k_1\sqrt{t} + \eta) \} - c_1 e^{k_1^2t} \{ 2\cosh(k_2z) - e^{-k_2z} \text{Erf}(\eta - k_2\sqrt{t}) - e^{k_2z} \text{Erf}(\eta + k_2\sqrt{t}) \} + \frac{1}{2} e^{(k_3^2 - k_1^2)t} \{ 2\cosh(k_3z) - e^{-k_3z} \text{Erf}(\eta - k_3\sqrt{t}) - e^{k_3z} \text{Erf}(\eta + k_3\sqrt{t}) \} + c_1 e^{k_5^2t} \{ 2\cosh(k_4z) + e^{-k_4z} \text{Erf}(k_5\sqrt{t} - k_6\eta) - e^{k_4z} \text{Erf}(k_5\sqrt{t} + k_6\eta) \} - 2c_1 \text{Erfc}(k_6\eta) + V_1(z, t) - V_1(z, t-1)H(t-1), \tag{31}$$

here
$$V_1(z, t) = L^{-1} \left\{ \frac{(A_1 + A_2)}{s^2(s - B_1)} \left(e^{-z\sqrt{R_aP_r}} - e^{-z\sqrt{b+s}} \right) \right\} + L^{-1} \left\{ \frac{aA_3}{s^2(s - B_2)} \left(e^{-z\sqrt{b+s}} - e^{-z\sqrt{sS_c}} \right) \right\} = -c_2 e^{k_{10}^2t} \{ 2\cosh(k_7z) - e^{-k_7z} \text{Erf}(\eta - k_7\sqrt{t}) - e^{k_7z} \text{Erf}(\eta + k_7\sqrt{t}) \} + (c_3t + c_4) \{ 2\cosh(k_1z) + e^{-k_1z} \text{Erf}(k_1\sqrt{t} - \eta) - e^{k_1z} \text{Erf}(k_1\sqrt{t} + \eta) \} + c_5z \{ 2\sinh(k_1z) + e^{-k_1z} \text{Erf}(k_1\sqrt{t} - \eta) - e^{k_1z} \text{Erf}(k_1\sqrt{t} + \eta) \} + c_6z\sqrt{t} e^{-k_8^2\eta^2} + c_2 e^{k_{10}^2t} \{ 2\cosh(k_9z) + e^{-k_9z} \text{Erf}(k_{10}\sqrt{t} - k_8\eta) - e^{k_9z} \text{Erf}(k_{10}\sqrt{t} + k_8\eta) \} - (c_7z^2 + c_8t + 2c_2) \text{Erfc}(k_8\eta) + c_9 e^{k_{5t}^2} \{ 2\cosh(k_2z) - e^{-k_2z} \text{Erf}(\eta - k_2\sqrt{t}) \}$$

$$-e^{k_2 z} \operatorname{Erf}(\eta + k_2 \sqrt{t})\} - c_{10} z \sqrt{t} e^{-k_6^2 \eta^2} - c_9 e^{k_5^2 t} \{2 \cosh(k_4 z) + e^{-k_4 z} \operatorname{Erf}(k_5 \sqrt{t} - k_6 \eta) - e^{k_4 z} \operatorname{Erf}(k_5 \sqrt{t} + k_6 \eta)\} + (c_{12} z^2 + c_{11} t + 2c_9) \operatorname{Erfc}(k_6 \eta).$$

Solution for an isothermal plate:

For the case of an isothermal plate, the solutions for concentration, temperature and velocity profiles are obtained as flows:

$$\theta_{iso}(z, t) = \operatorname{Erfc}(k_8 \eta) \tag{32}$$

$$\phi_{iso}(z, t) = (1 - a) \operatorname{Erfc}(k_6 \eta) + a \operatorname{Erfc}(k_8 \eta) \tag{33}$$

$$V_{iso}(z, t) = (c_1 + c_3) \{2 \cosh(k_1 z) + e^{-k_1 z} \operatorname{Erf}(k_1 \sqrt{t} - \eta) - e^{k_1 z} \operatorname{Erf}(k_1 \sqrt{t} + \eta)\} - \frac{c_8}{2} e^{k_{10}^2 t} \{2 \cosh(k_7 z) - e^{-k_7 z} \operatorname{Erf}(\eta - k_7 \sqrt{t}) - e^{k_7 z} \operatorname{Erf}(\eta + k_7 \sqrt{t})\} - (1 - a) c_1 e^{k_5^2 t} \{2 \cosh(k_2 z) - e^{-k_2 z} \operatorname{Erf}(\eta - k_2 \sqrt{t}) - e^{k_2 z} \operatorname{Erf}(\eta + k_2 \sqrt{t})\} + \frac{1}{2} e^{(k_3^2 - k_1^2) t} \{2 \cosh(k_3 z) - e^{-k_3 z} \operatorname{Erf}(\eta - k_3 \sqrt{t}) - e^{k_3 z} \operatorname{Erf}(\eta + k_3 \sqrt{t})\} + \frac{c_8}{2} e^{k_{10}^2 t} \{2 \cosh(k_9 z) + e^{-k_9 z} \operatorname{Erf}(k_{10} \sqrt{t} - k_8 \eta) - e^{k_9 z} \operatorname{Erf}(k_{10} \sqrt{t} + k_8 \eta)\} - c_8 \operatorname{Erfc}(k_8 \eta) - 2c_1 (1 - a) \operatorname{Erfc}(k_6 \eta) + (1 - a) c_1 e^{k_5^2 t} \{2 \cosh(k_4 z) + e^{-k_4 z} \operatorname{Erf}(k_5 \sqrt{t} - k_6 \eta) - e^{k_4 z} \operatorname{Erf}(k_5 \sqrt{t} + k_6 \eta)\}, \tag{34}$$

here

$$b = \frac{M i}{m + i} + 2i\Omega + \frac{1}{K}, R_a = \frac{3R}{3R + 4}, a = \frac{P_r S_r S_c R_a}{S_c - P_r R_a}, A_1 = \frac{G_r}{1 - P_r R_a}, A_2 = \frac{a G_m}{1 - P_r R_a}, A_3 = \frac{G_m}{1 - S_c},$$

$$B_1 = \frac{b}{P_r R_a - 1}, B_2 = \frac{b}{S_c - 1}, c_1 = \frac{A_3}{2B_2}, c_2 = \frac{A_1 + A_2}{2B_1^2}, c_3 = \frac{A_1 + A_2}{2B_1} - \frac{aA_3}{2B_2}, c_4 = \frac{A_1 + A_2}{2B_1^2} - \frac{aA_3}{2B_2^2},$$

$$c_5 = \frac{A_1 + A_2}{4B_1 \sqrt{b}} - \frac{aA_3}{4B_2 \sqrt{b}}, c_6 = \frac{\sqrt{P_r R_a} (A_1 + A_2)}{B_1 \sqrt{\pi}}, c_7 = \frac{P_r R_a (A_1 + A_2)}{2B_1}, c_8 = \frac{A_1 + A_2}{B_1}, c_9 = \frac{aA_3}{2B_2^2},$$

$$c_{10} = \frac{aA_3}{B_2} \sqrt{\frac{S_c}{\pi}}, c_{11} = \frac{aA_3}{B_2}, c_{12} = \frac{aA_3 S_c}{2B_2}, k_1 = \sqrt{b}, k_2 = \sqrt{b + B_2}, k_3 = \sqrt{b - \lambda}, k_4 = \sqrt{B_2 S_c},$$

$$k_5 = \sqrt{B_2}, k_6 = \sqrt{S_c}, k_7 = \sqrt{b + B_1}, k_8 = \sqrt{P_r R_a}, k_9 = \sqrt{B_1 P_r R_a}, k_{10} = \sqrt{B_1}, \eta = \frac{z}{2\sqrt{t}}$$

Skin friction coefficient, Sherwood Number and Nusselt number:

The shear stress components in the primary and secondary directions are obtained by

$$\tau_x = -\mu \frac{\partial u}{\partial z} \quad \text{and} \quad \tau_y = -\mu \frac{\partial v}{\partial z} \quad \text{respectively.}$$

By using non-dimensional parameters given in (9), the dimensionless stresses are

$$\tau_1(z', t') = \frac{\tau_x}{\tau_o} = -\frac{\partial u'}{\partial z'} \quad \text{and} \quad \tau_2(z', t') = \frac{\tau_y}{\tau_o} = -\frac{\partial v'}{\partial z'} \quad \text{where } \tau_o = \rho u_o^2.$$

Consider the complex notation i.e. $\tau(z', t') = \tau_1(z', t') + i\tau_2(z', t')$ and after omitting the prime ('), the non-dimensional shear stress changes to:

$$\tau(z, t) = \tau_1(z, t) + i\tau_2(z, t) = -\frac{\partial V(z, t)}{\partial z}$$

Therefore, the non-dimensional coefficients of skin friction at the plate in complex form is given as

$$\begin{aligned} [S_f(t)]_{ramped} &= \tau(0, t) \\ &= \frac{1}{\sqrt{\pi t}} \left(2c_1 e^{-k_1^2 t} + e^{-k_1^2 t} - 2c_1 e^{(k_5^2 - k_2^2)t} \right) + 2c_1 k_1 \operatorname{erf}(k_1 \sqrt{t}) - 2c_1 k_2 e^{k_5^2 t} \operatorname{erf}(k_2 \sqrt{t}) \\ &+ k_3 e^{(k_3^2 - k_1^2)t} \operatorname{erf}(k_3 \sqrt{t}) + 2c_1 k_4 e^{k_5^2 t} \operatorname{erf}(k_5 \sqrt{t}) + S_1(t) - S_1(t-1)H(t-1), \end{aligned} \tag{35}$$

where $S_1(t) = \frac{1}{\sqrt{\pi t}} \{ 2(c_3 t + c_4) e^{-k_1^2 t} + 2c_9 e^{(k_5^2 - k_2^2)t} + (k_6 c_{11} - k_8 c_8) t - 2c_2 e^{(k_{10}^2 - k_7^2)t} \}$

$$\begin{aligned} &+ (c_{10} - c_6) \sqrt{t} + \{ 2k_1(c_3 t + c_4) + 2c_5 \} \operatorname{erf}(k_1 \sqrt{t}) + 2c_9 k_2 e^{k_5^2 t} \operatorname{erf}(k_2 \sqrt{t}) \\ &- 2c_9 k_4 e^{k_5^2 t} \operatorname{erf}(k_5 \sqrt{t}) - 2c_2 k_7 e^{k_{10}^2 t} \operatorname{erf}(k_7 \sqrt{t}) + 2c_2 k_9 e^{k_{10}^2 t} \operatorname{erf}(k_{10} \sqrt{t}). \end{aligned}$$

$$\begin{aligned} [S_f(t)]_{iso} &= \tau(0, t) = \frac{1}{\sqrt{\pi t}} \{ (2c_1 + 2c_3 + 1) e^{-k_1^2 t} - 2c_1(1-a) e^{(k_5^2 - k_2^2)t} - c_8 e^{(k_{10}^2 - k_7^2)t} \} \\ &+ 2k_1(c_1 + c_3) \operatorname{erf}(k_1 \sqrt{t}) - 2c_1 k_2(1-a) e^{k_5^2 t} \operatorname{erf}(k_2 \sqrt{t}) + k_3 e^{(k_3^2 - k_1^2)t} \operatorname{erf}(k_3 \sqrt{t}) \\ &+ 2c_1 k_4(1-a) e^{k_5^2 t} \operatorname{erf}(k_5 \sqrt{t}) - c_8 k_7 e^{k_{10}^2 t} \operatorname{erf}(k_7 \sqrt{t}) + c_8 k_9 e^{k_{10}^2 t} \operatorname{erf}(k_{10} \sqrt{t}) \end{aligned} \tag{36}$$

Hence, the non-dimensional coefficients of skin friction in the primary and secondary directions respectively can be found as:

$$S_{f_x} = \operatorname{Re}(S_f) \quad \text{and} \quad S_{f_y} = \operatorname{Im}(S_f)$$

Again, by using (9), non-dimensional Sherwood and Nusselt number are obtained as follows:

Sherwood number

$$[Sh]_{ramped} = -\left(\frac{\partial \phi}{\partial z}\right)_{z=0} = \sqrt{\frac{S_c}{\pi t}} + \frac{2a}{\sqrt{\pi}} \left(\sqrt{P_r R_a} - \sqrt{S_c}\right) \left\{\sqrt{t} - \sqrt{t-1} H(t-1)\right\} \quad (37)$$

$$[Sh]_{iso} = -\left(\frac{\partial \phi}{\partial z}\right)_{z=0} = \frac{1}{\sqrt{\pi t}} \left\{a\sqrt{P_r R_a} + (1-a)\sqrt{S_c}\right\} \quad (38)$$

Nusselt number

$$[N_u]_{ramped} = -\left(\frac{\partial \theta}{\partial z}\right)_{z=0} = 2\sqrt{\frac{P_r R_a t}{\pi}} - 2\sqrt{\frac{P_r R_a (t-1)}{\pi}} H(t-1) \quad (39)$$

$$[N_u]_{iso} = -\left(\frac{\partial \theta}{\partial z}\right)_{z=0} = \sqrt{\frac{P_r R_a}{\pi t}} \quad (40)$$

3. RESULTS AND DISCUSSION

In order to display the physical changes of some parameters of interest on the obtained solution, the numerical results for temperature, velocity, concentration, Nusselt number, Skin friction, Sherwood number are computed and shown graphically in Figs.1– 21. The Figs.1–10 reveals the variation in the magnitude of primary and secondary fluid velocities in the boundary layer region versus boundary layer coordinate for various values of Soret number S_r , permeability parameter K , Hall parameter m , rotation parameter Ω , exponential parameter λ , radiation parameter R taking $P_r = 0.71$, $S_c = 2.01$, $t = 0.4$, $G_r = 5$ and $G_m = 5$. For both isothermal and ramped temperature plates; it is noticed that, primary fluid velocity u (velocity along plate) and secondary fluid velocity v (velocity transverse to plate) acquire a different maximum value in the vicinity of the plate and then decrease gradually to approach free stream value.

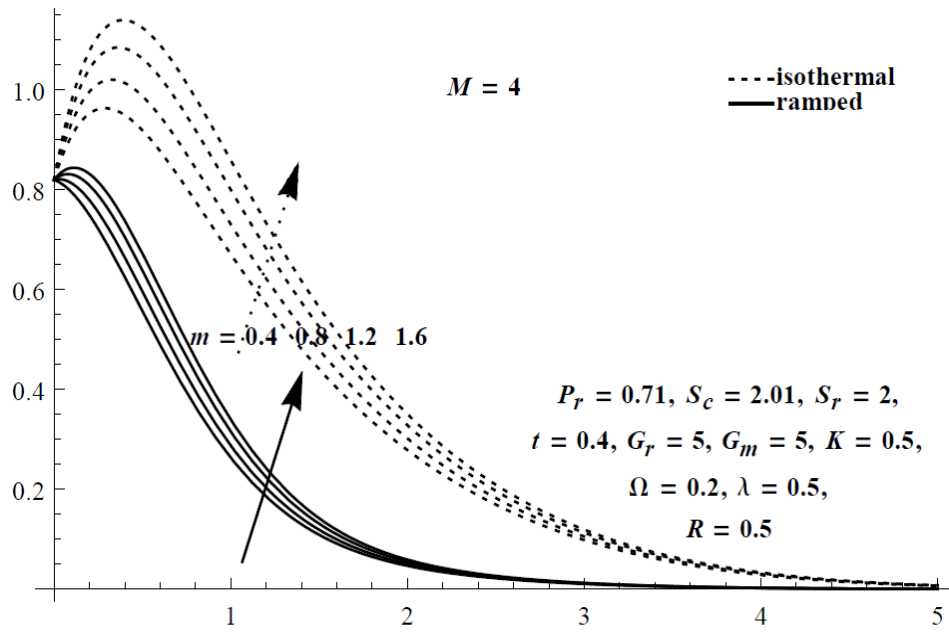


Fig.1.Primary Velocity profile for $m (<2)$

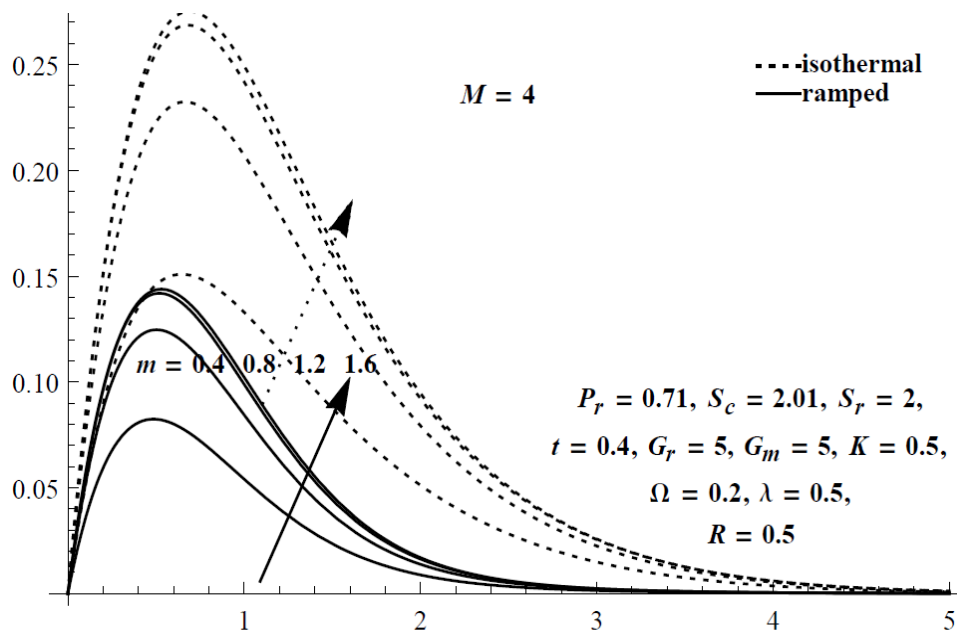


Fig.2.Secondary Velocity profile for $m (<2)$

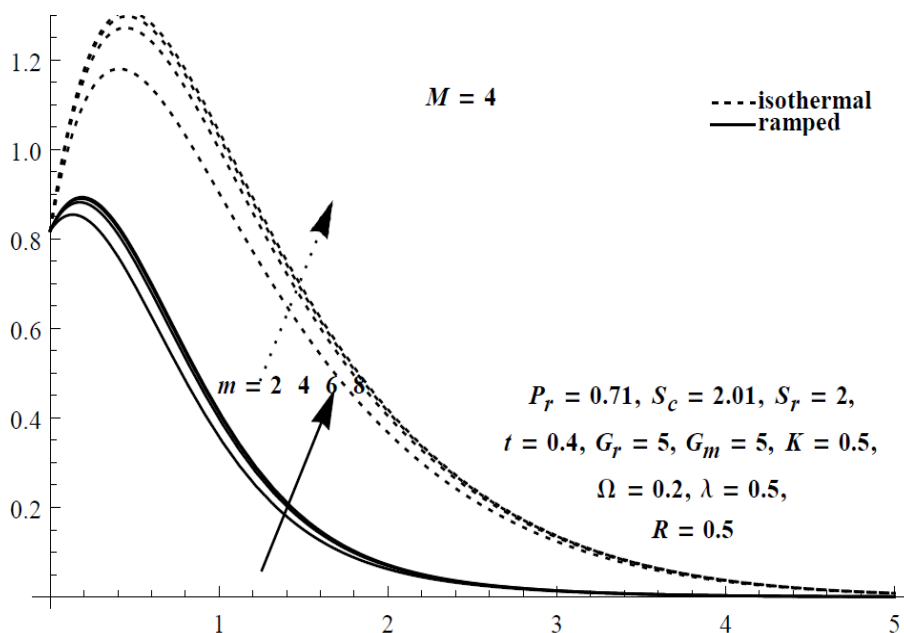


Fig.3. Primary Velocity profile for $m (>2)$

The effect of Hall parameter on the fluid velocity is depicted in Figs.1–4. An interesting result is noticed that the magnitude of secondary velocity increases with the increase of Hall parameter $m < 2$ and the velocity gradually decreases for $m > 2$. This may be attributed to the fact that the value of the term $1/(1+m^2)$ is very small for large value of m ; hence large m diminishes the resistive effect of the applied magnetic field. The primary velocity increases with the increase in m (for any value of m).

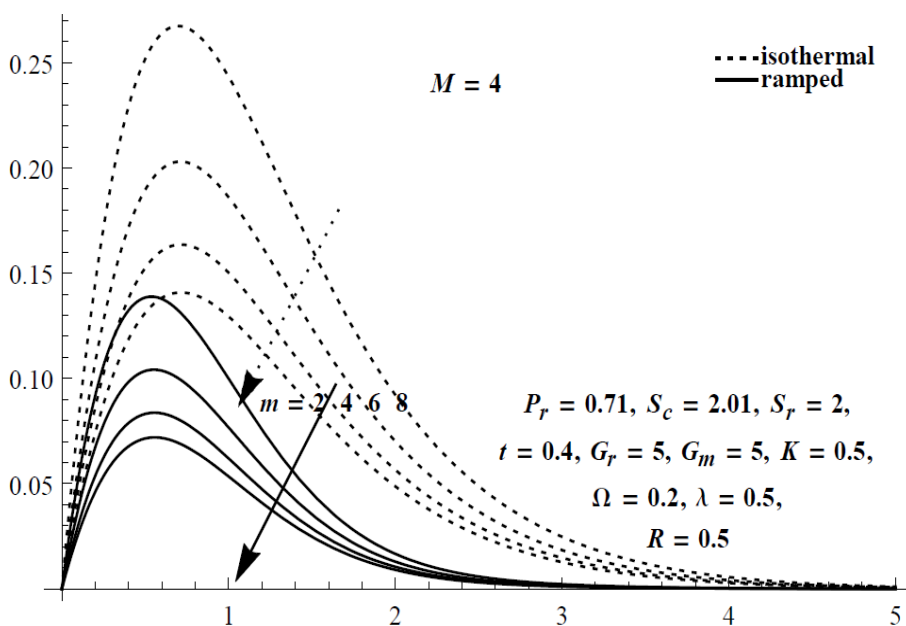


Fig.4. Secondary Velocity profile for $m (>2)$

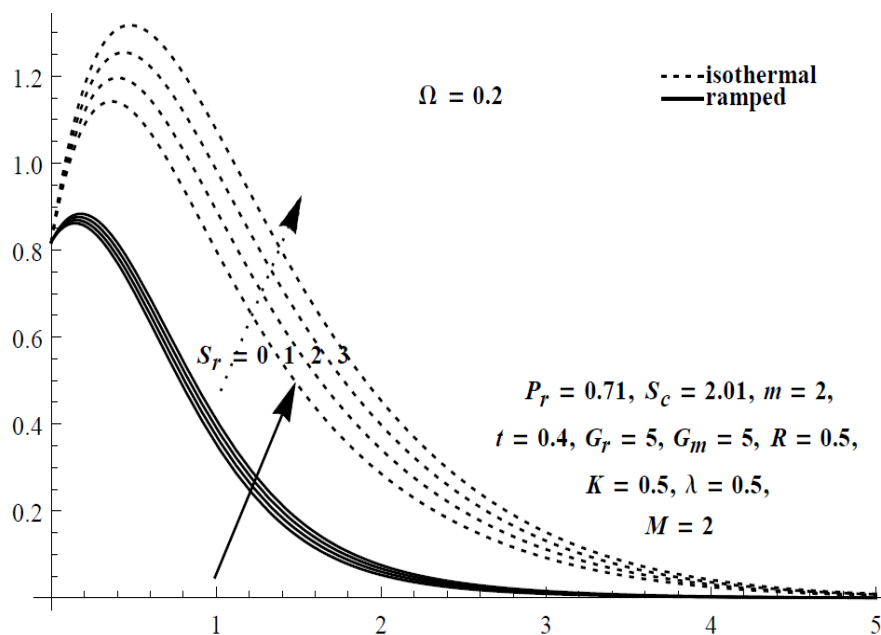


Fig.5. Primary Velocity profile for S_r

Figs.5–6 displays the influence of Soret number S_r on the velocity profiles and it is observed that primary as well as secondary fluid velocity increases with the increase in S_r . Furthermore, the effect of rotation, permeability and magnetic parameters can be seen from Figs.7–8. It is noticed that for both isothermal and ramped temperature plates, the primary fluid velocity decreases and secondary fluid velocity increases with increase in the rotation parameter. Hence rotation has tendency to accelerate the secondary flow and retards the flow in the primary direction. Physically it is in agreement with the Coriolis force which has a tendency to enhance the secondary flow and suppress the primary flow. While, both the components of the velocity increases with the increase in the permeability parameter K ; a porous medium with large value of permeability parameter will support the movement of the fluid through it. It also reveals that an increase in the magnetic parameter M can decrease the primary and increase the secondary fluid velocities. Physically it is due to the fact that if we apply a transverse magnetic field towards the flow, it will offer a Lorentz force which acts in the transverse direction and hence resists the primary flow. It is also evident from Figs. 9–10 and Fig. 16 that both the primary and secondary velocities as well as temperature decrease with

the increase in the radiation parameter R . Whereas we noticed in the Figs.11–13 that concentration within the boundary layer decreases with increase in S_c and it increases with increase in S_r or t for both isothermal and ramped temperature plates. Also, temperature of the system reduces with time (Fig.15).

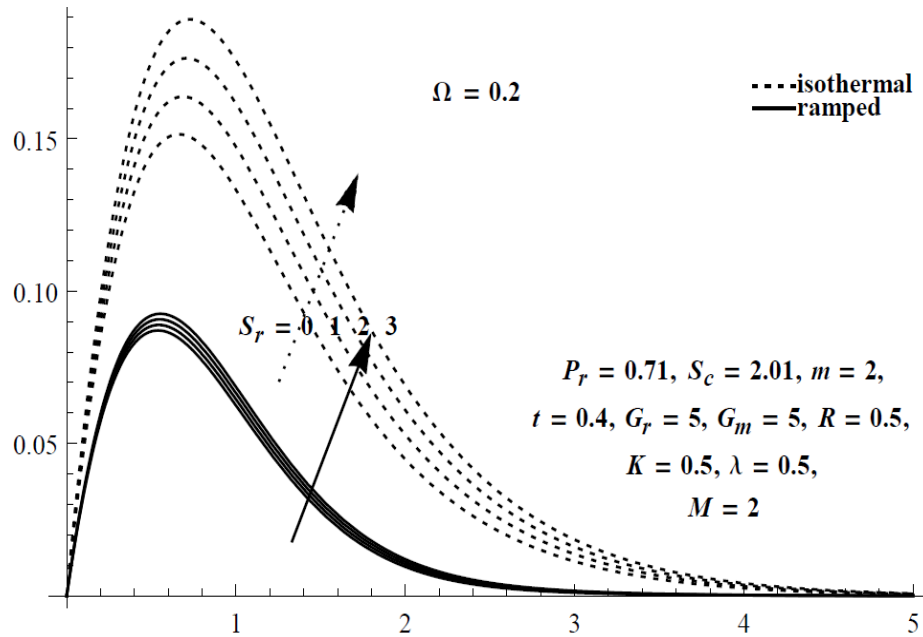


Fig.6. Secondary Velocity profile for S_r

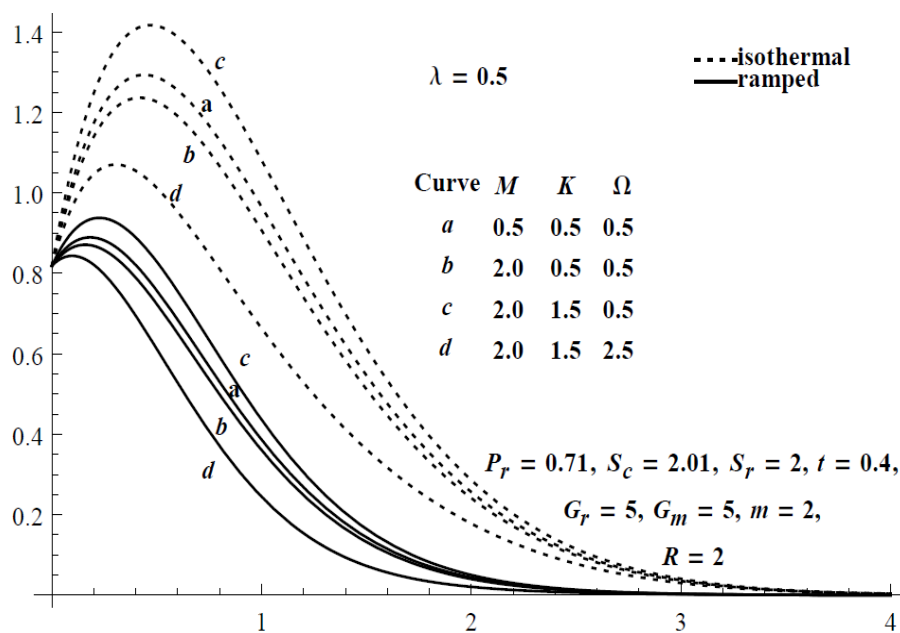


Fig.7. Primary Velocity profile for M, K and Ω

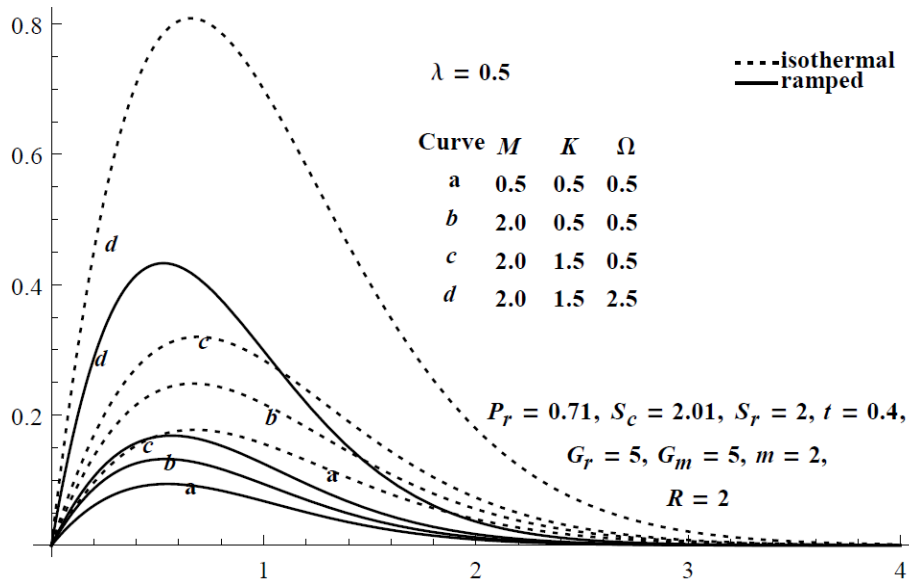


Fig.8. Secondary Velocity profile for M, K and Ω

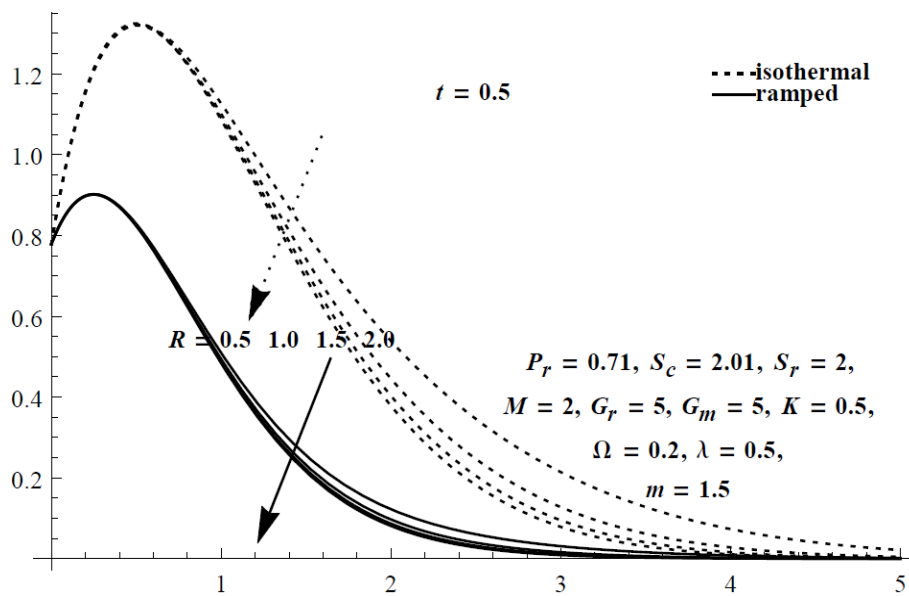


Fig.9. Primary Velocity profile for R

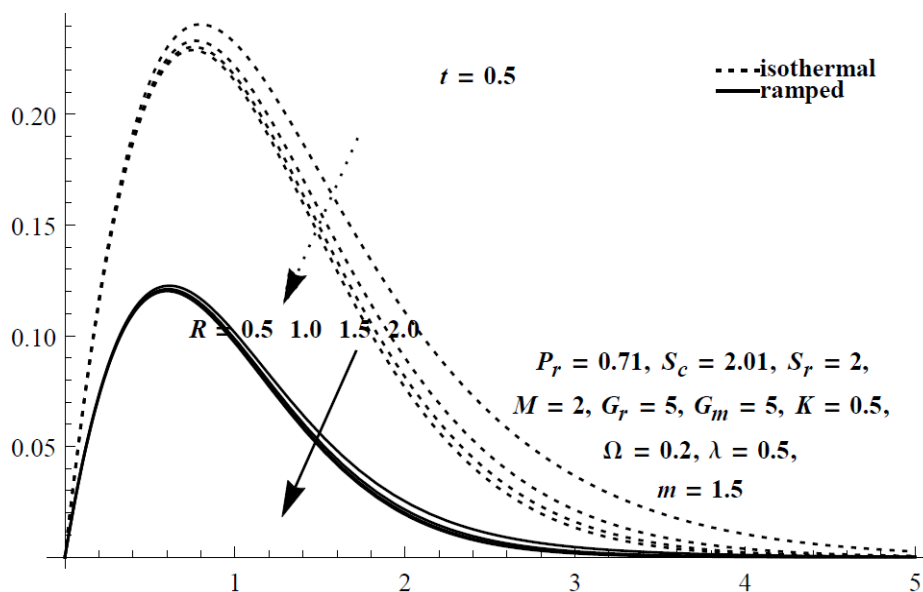


Fig.10. Secondary Velocity profile for R

For both isothermal and ramped temperature plates, the influence of different governing parameters on Sherwood number Sh , Nusselt number N_u and skin-friction coefficient are shown in Figs. 16–21. From Figs.16–17 it is evident that, the primary skin friction i.e. S_{fx} and magnitude of secondary skin friction i.e. S_{fy} increase on increasing either M or Ω , whereas these decrease with the increase in exponent parameter λ . Furthermore, S_{fx} decreases and magnitude of S_{fy} increases with the increase in porosity parameter K .

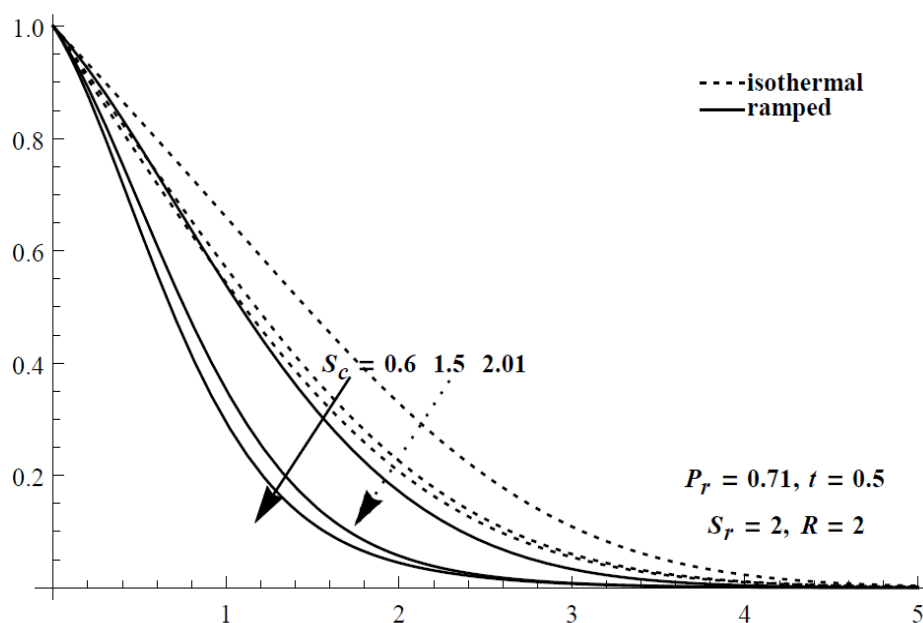


Fig.11. Concentration profile for S_c

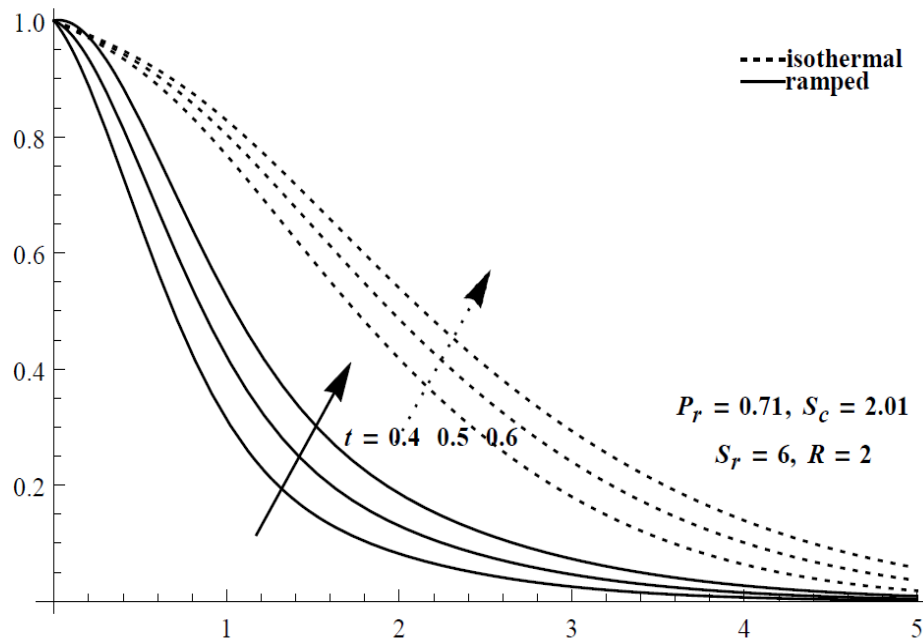


Fig.12.Concentration profile for t

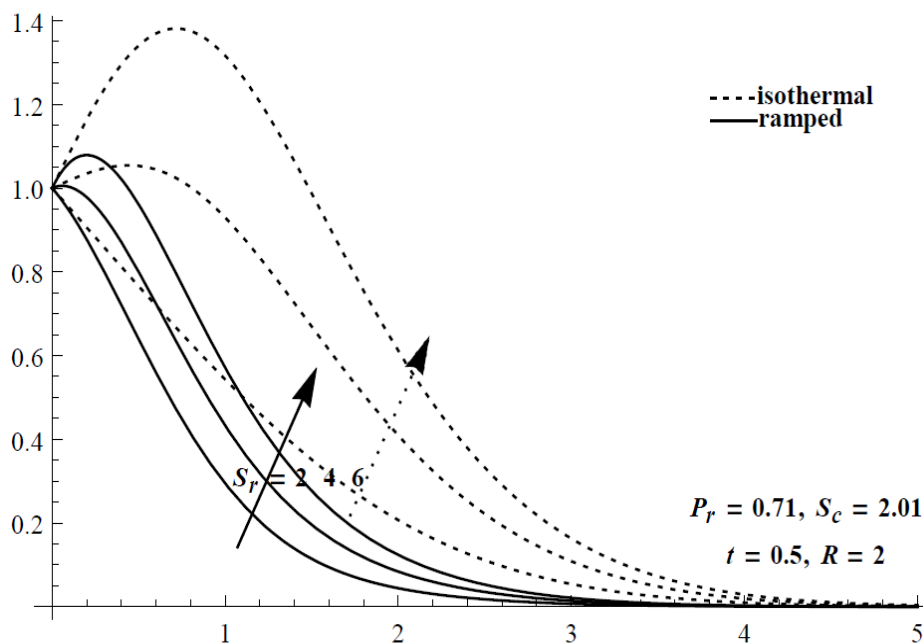


Fig.13.Concentration profile for S_r

Nusselt number N_u measure the heat transfer rate at the plate and Figs.20 – 21 depicts the changes in the values of Nusselt number with Prandtl number and radiation parameter. For both isothermal and ramped temperature plates, Nusselt number increases on increasing P_r or R . Further, for isothermal plate, N_u decreases with the increase in time. On the other hand, for ramped temperature, it increases on increasing t . The rate of mass transfer is measured by

Sherwood number Sh and Figs.18–19 reveals variation in Sh with the solet number and radiation, for both isothermal and ramped temperature plates; it is found that Sh decreases with increase in $S_r / R / t$.

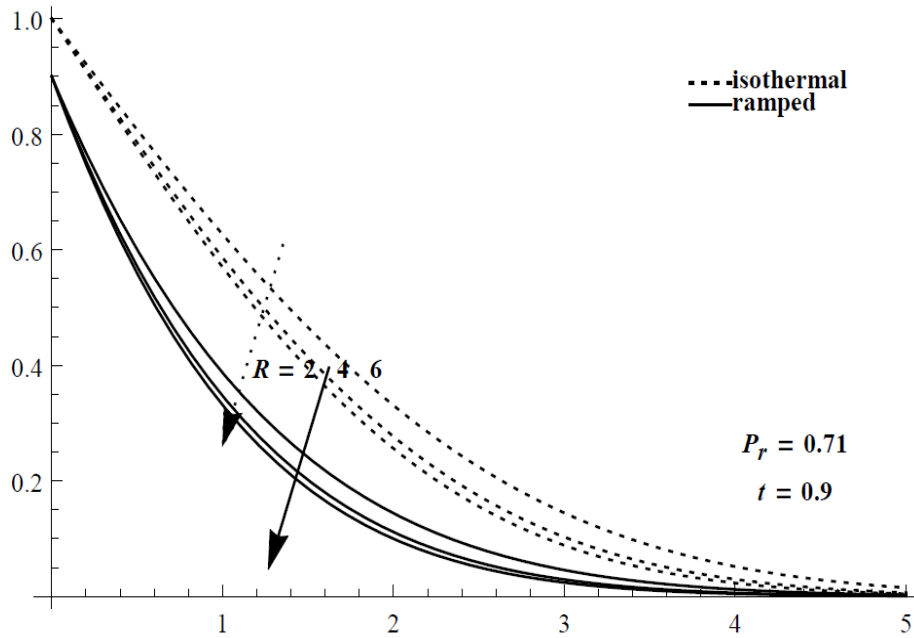


Fig.14. Temperature profile for R

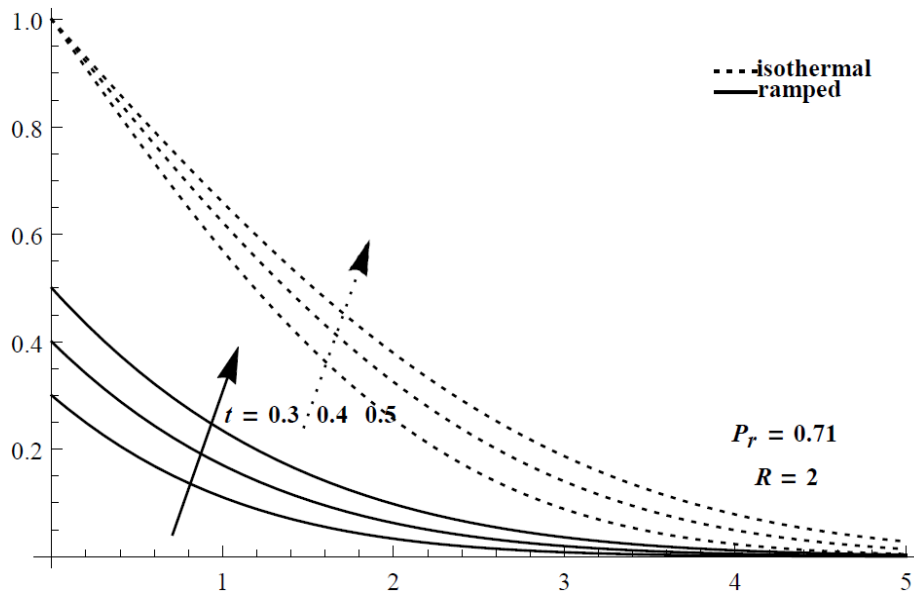


Fig.15. Temperature profile for t

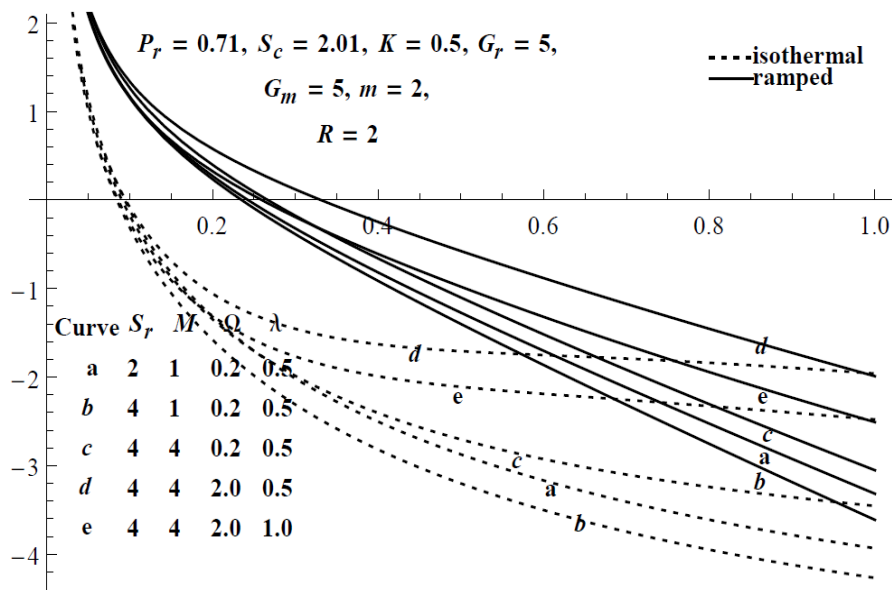


Fig.16. Primary Skin Friction profile

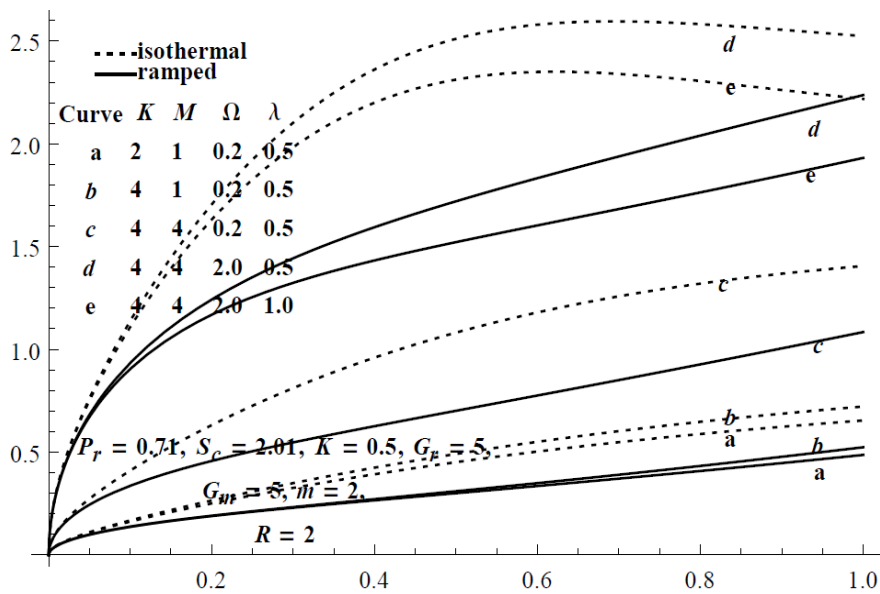


Fig.17. Secondary Skin Friction profile

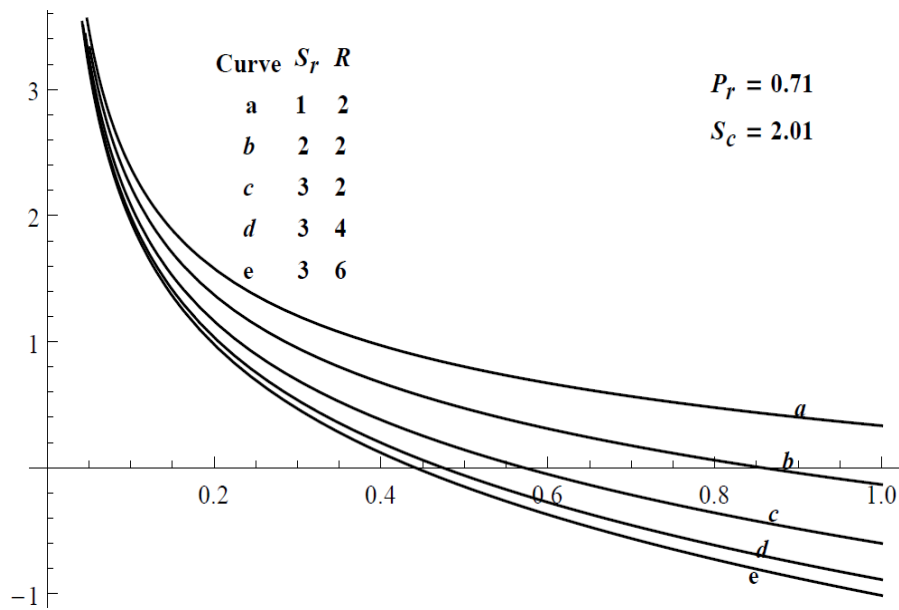


Fig.18. Sherwood Number profile for ramped plate temperature with time

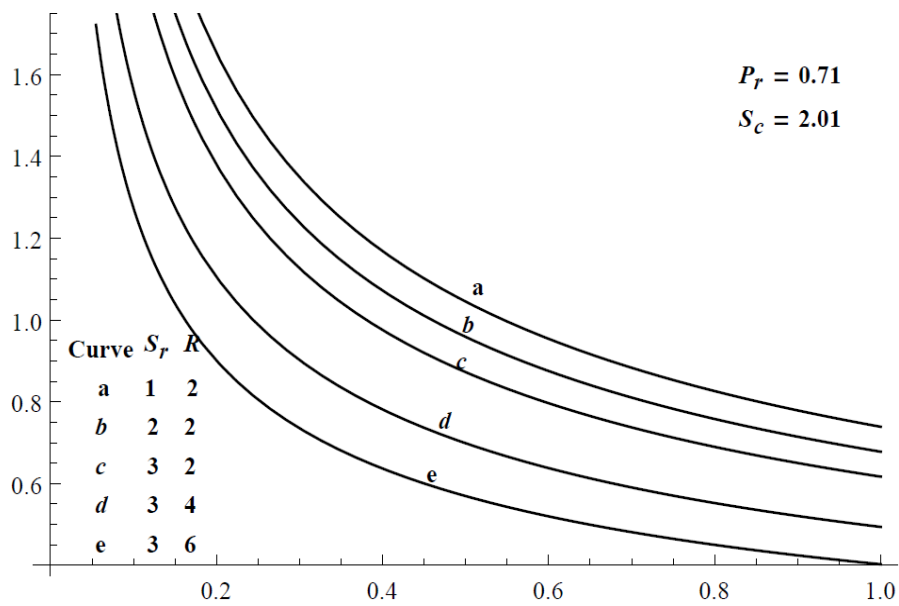


Fig.19. Sherwood Number profile for isothermal plate temperature with time

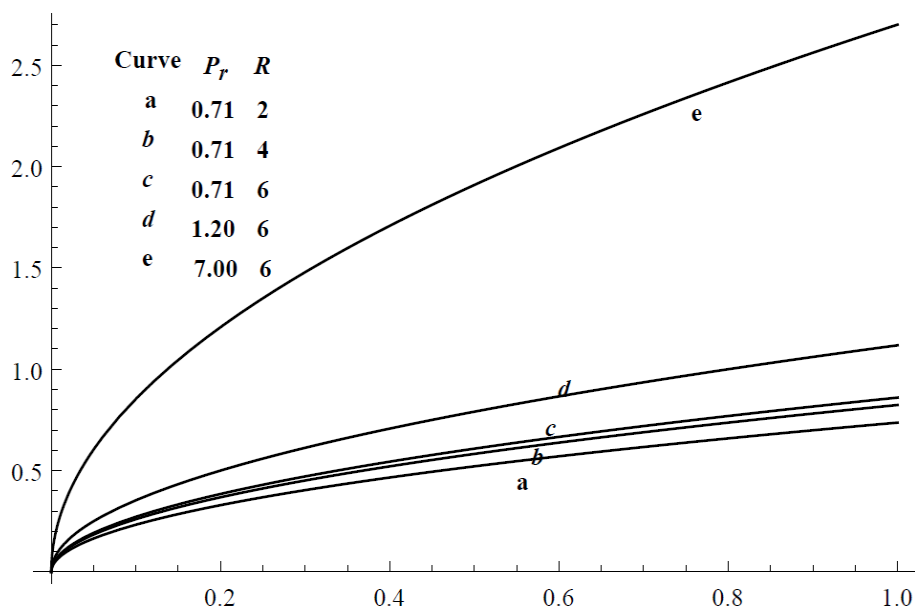


Fig.20.Nusselt Number profile for Ramped plate temperature with time

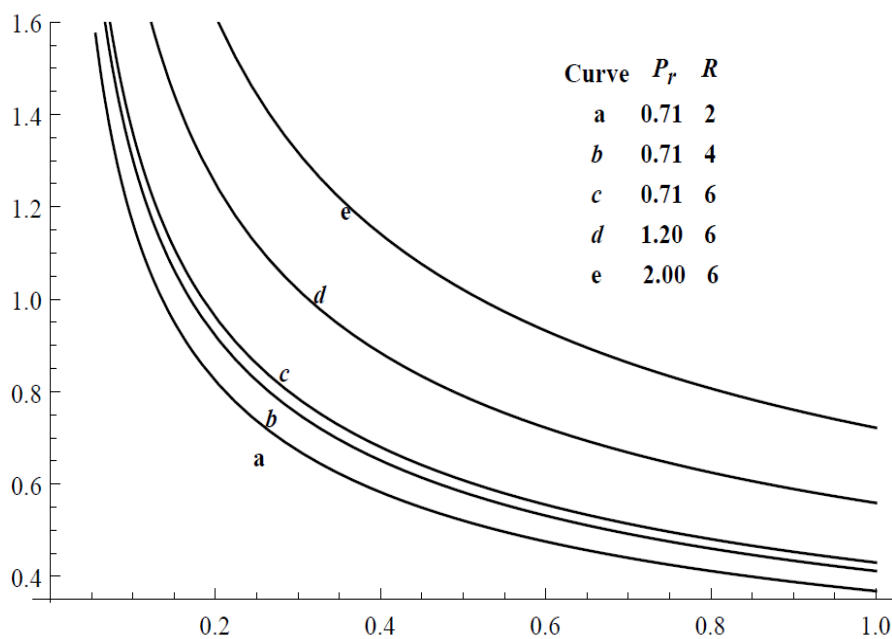


Fig.21.Nusselt Number profile for Isothermal plate with time

4. CONCLUSION

It is observed that after a certain magnetic field strength the flow behaviour in the boundary layer is significantly affected with Hall parameter. For both isothermal and ramped temperature plates, Hall currents has tendency to accelerate the primary fluid velocity; while

it accelerate the secondary fluid velocity for $m < m_0$, and decelerate for $m > m_0$, where m_0 depends on M . Other conclusions are as follows:

- The amplitude of temperature, velocity and concentration fields for isothermal plate are always larger than ramped plate temperature.
- Larger value of rotation and magnetic field decrease the primary fluid velocity, and increase the magnitude of secondary fluid velocity.
- The magnitude of dimensionless velocities increase with an increase in the permeability of porous medium.
- Temperature and magnitude of dimensionless velocities of the fluid decrease with increase of radiation parameter.
- The increase in either Soret number or radiation or time causes the decrease in Sherwood number.

5. REFERENCES

- [1] Agarwal, H.L., P.C. Ram, and V. Singh (1983). Combined effect of dissipation and Hall effect on free convective in a rotating fluid. *Indian J. Pure ppl. Math.* 14(3), 314-32.
- [2] Alam, M.S., and M.M. Rahman (2006). Dufour and Soret effects on mixed convection flow past a vertical porous flat plate with variable suction. *Nonlinear Analysis: Modelling and Control* 11(1), 3-12.
- [3] Anghel, M., H. S. Takhar, I. Pop (2000). Dufour and Soret effects on free convection boundary-layer over a vertical surface embedded in a porous medium. *Studia Universitatis Babes-Bolyai. Mathematica* XLV (4), 11-21.
- [4] Beg, O.A., T. A. Beg, A.Y. Bakier, and V.R. Prasad (2009). Chemically-reacting mixed convective heat and mass transfer along inclined and vertical plates with Soret and Dufour effects: Numerical solutions. *Int. J. Applied Mathematics and Mechanics* 5(2), 39-57.
- [5] Bhargava, R., R. Sharma and O. A. Beg (2009). Oscillatory chemically-reacting MHD free convection heat and mass transfer in a porous medium with Soret and Dufour effects: finite element modelling. *Int. J. Applied Mathematics and Mechanics* 5(6), 15-37.
- [6] Branover, H. (1978). *Magnetohydrodynamic Flow in Ducts*. John Wiley and Sons, New

York.

- [7] Chamkha, A. J. (2000). Thermal radiation and buoyancy effects on hydromagnetic flow over an accelerating permeable surface with heat source or sink. *International Journal of Engineering Sciences* 38, 1699 -1712.
- [8] Cowling, T.G. (1957). *Magnetohydrodynamics*. Interscience, New York.
- [9] Ganesan, P., and P. Laganathan (2002). Radiation and mass transfer effects on flow of an incompressible viscous fluid past a moving cylinder. *Int. J. of Heat and Mass Transfer* 45, 4281-4288.
- [10] Greenspan, H. P. (1968). *The Theory of Rotating Fluids*, Cambridge University Press, London.
- [11] Hossain, M.A. and H.S. Takhar (1996). Radiation effect on mixed convection along a vertical plate with uniform surface temperature. *Heat and Mass Transfer* 31, 243-248.
- [12] Ibrahim, A.A. (2009). Analytic solution of heat and mass transfer over a permeable stretching plate affected by chemical reaction, internal heating, Dufour-Soret effect and Hall effect. *Thermal science* 13 (2), 183-197.
- [13] Jaimala, Vikrant and K. Vivek (2013). Thermal convection in a Couple-Stress fluid in the presence of horizontal magnetic field with Hall currents. *Application and applied Mathematics* 8(1), 161-117.
- [14] Kafoussias, N. G., and E.W. Williams (1995). Thermal-diffusion and diffusion-thermo effects on mixed free-forced convective and mass transfer boundary layer flow with temperature dependent viscosity. *International Journal of Engineering Science* 33(9), 1369-1384.
- [15] Kim, Y.J. (2004). Heat and mass transfer in MHD Micropolar flow over a vertical moving porous plate in a porous medium. *Transport in Porous Media* 56(1), 17–37.
- [16] Makinde, O. D. (2011). MHD mixed convection with Soret and Dufour effects past a vertical plate embedded in a porous medium. *Latin American Applied Research* 41, 63-68.
- [17] Makinde, O.D., and P.Y. Mhone (2005). Heat transfer to MHD oscillatory flow in a channel filled with porous medium. *Romania Journal of Physics* 50(9-10), 931–938.

-
- [18] Mazumdar, B.S., A.S. Gupta, and N. datta (1976). Flow and heat transfer in hydrodynamic ekman layer on a porous plate with Hall effects. *Int. J. heat mass Transfer* 19, 523.
- [19] Muthucumaraswamy, R., and K. M. A. Prema (2016). Hall effects on flow past an exponentially accelerated infinite isothermal vertical plate with mass diffusion. *J. of App. Fluid Mech.*9(2), 889-897.
- [20] Muthucumaraswamy, R., N. Dhanasekar, and G. E. Prasad (2013). Rotation effects on unsteady flow past an accelerated isothermal vertical plate with variable mass transfer in the presence of chemical reaction of first order. *Journal of Applied Fluid Mechanics* 6 (4), 485 – 490.
- [21] Muthucumaraswamy, R., P. Ganesan, and V.M. Soundalgeker (2001). Heat and mass transfer effect on flow past impulsively started vertical plate. *Acta Mechanica* 146 (1), 1-8.
- [22] Osalusi, E., and P. Sibanda (2006). On variable laminar convection flow properties due to a porous rotating disk in a magnetic field. *Romania Journal of Physics* 51(9-10), 937 – 950.
- [23] Owen, J. M., and R. H. Rogers (1989). *Flow and heat transfer in rotating disc systems, Vol. I, Rotor - Stator Systems*, John Wiley Sons, New York.
- [24] Platten, J.K.(2006). The Soret effect: A review of recent experimental results. *Journal of applied mechanics* 73, 5-15.
- [25] Postelnicu, A. (2004). Influence of a magnetic field on heat and mass transfer by natural convection from vertical surfaces in porous media considering Soret and Dufour effects. *Int. J. Heat & Mas Transfer* 47, 1467-1472.
- [26] Postelnicu, A. (2007). Influence of chemical reaction on heat and mass transfer by natural convection from vertical surfaces in porous media considering Soret and Dufour effects. *Heat Mass Transfer* 43, 595-602.
- [27] Prasad, V.R., N.B. Reddy, and R. Muthucumaraswamy (2007). Radiation and mass transfer effects on two-dimensional flow past an impulsively started infinite vertical plate. *International Journal of Thermal Sciences* 46, 1251-1258.

- [28] Rajput, U.S., and Shareef, M.(2017). Unsteady MHD flow along exponentially accelerated vertical flat surface through porous medium with variable temperature and Hall current in a rotating system. *Journal of Fundamental and Applied Sciences* 9(2), 1050-1062.
- [29] Raptis, A. (1998). Radiation and free convection flow through a porous medium. *Int. Comm. Heat Mass Transfer* 25, 289-295.
- [30] Raptis, A., and C.V. Massalas (1998). Magnetohydrodynamic flow past a plate by the presence of radiation. *Heat and Mass Transfer* 34, 107-109.
- [31] Raptis, N., and N.G. Kafousias (1982). Magnetohydrodynamic free convection flow and mass transfer through porous medium bounded by an infinite vertical porous plate with constant heat flux. *Can. J. Physics* 60(12), 1725-1729.
- [32] Sattar, M. A. (1993). Unsteady hydromagnetic free convection flow with Hall current, mass transfer and variable suction through a porous medium near an infinite vertical porous plate with constant heat flux. *Int. J. Energy Research* 17, 1-5.
- [33] Soong, C. Y. (2001). Thermal buoyancy effects in rotating non-isothermal flows, *Int. J. Rotating Machinery* 7(6), 435-446.
- [34] Soong, C. Y., and H. L. Ma (1995). Unsteady analysis of non-isothermal flow and heat transfer between rotating co-axial disks, *Int. J. of Heat and Mass Transfer* 38(10), 1865-1878.
- [35] Soundalgekar, V. M. (1979). Effects of Mass Transfer and free-convection currents on the flow past an impulsively started vertical plate. *J. Appl. Mech* 46(4), 757-760.
- [36] Takhar, H.S., A.J. Chamkha, and G. Nath (2001).Unsteady laminar MHD flow and heat transfer in the stagnation region of an impulsively spinning and translating sphere in the presence of buoyancy forces. *International Journal of Heat and Mass Transfer* 37, 397-402.
- [37] Takhar, H.S., R.S.R. Gorla, and V.M. Soundalgekar (1996). Radiative effects on MHD free convection flow of a gas past a semi-infinite vertical plate. *International Journal of Numerical Heat Fluid Flow* 2(2), 77-83.

How to cite this article:

RajputUS, Shareef M. Study of hall and soret effect on mhd flow with a ramped plate temperature of an exponentially accelerated vertical plate embedded in a porous medium. *J. Fundam. Appl. Sci.*, 2019, 11(1), 385-411.